• Human Brain Mapping 3:56–65(1995) •

Regulation of rCBF by Diffusible Signals: An Analysis of Constraints on Diffusion and Elimination

K.J. Friston

The Wellcome Department of Cognitive Neurology, Queen Square, and the MRC Cyclotron Unit, Hammersmith Hospital, London, United Kingdom

Abstract: Local changes in cerebral hemodynamics are observed within a few hundred milliseconds of changes in neural activity. If hemodynamic responses are mediated by passive diffusion of a spatial signal (from the site of neural activity to the microvessels) then the dynamics of the response suggest a lower limit on the signal's apparent diffusion and elimination. The aim of this work was to estimate these limits and narrow the field of possible candidate substances.

A simple biophysical simulation was used to examine how the time course of concentration changes in a spatial signal, at the site of action (microvessels), depends on key diffusion parameters (source geometry, apparent diffusion and elimination half-life). The simulations suggested 1) that the rise in signal concentration is mostly a function of source geometry and diffusion. Conversely falls in concentration depend on elimination and 2) even when sources are very sparsely distributed Nitric Oxide would have a sufficiently fast diffusion and elimination to signal the early components of activity-dependent hemodynamic response by passive diffusion.

Key words: hemodynamics, nitric oxide, diffusion, elimination, spatial signalling, regional cerebral blood flow, neural activity

INTRODUCTION

This paper concerns the regulation of local hemodynamics in the brain. Understanding the nature of activity-dependent hemodynamic changes is becoming increasingly important with the advent of imaging techniques [e.g. intrinsic signal optical imaging, near infra-red imaging, functional magnetic resonance imaging (fMRI) and positron emission tomography (PET)] that use transient hemodynamic responses to map the functional organization of the brain [e.g. Masino et al., 1993; Kwong et al., 1992]. The aim of this work was to characterize the constraints on diffusion and elimination of any substance that is capable of coupling neural activation and blood flow changes by passive diffusion. This characterisation used a simple biophysical simulation based on empirical estimates of relevant anatomical and diffusion parameters.

Diffusing substances can be classified by their roles as *informational* or *energetic* [Nicholson and Rice, 1991]. This paper is concerned with the diffusional behavior of putative informational substances that mediate or modulate vasodilation by diffusing from the site of neural activity, within the neural parenchyma, to sites of action in the microvessels.

NO and the regulation of cerebral perfusion

The mechanisms regulating cerebral perfusion, during neural activation, have been studied for many decades. Roy and Sherrington [1890] proposed that

Received for publication May 20, 1994; revision accepted May 4, 1995.

Address reprint requests to K.J. Friston, MRC Cyclotron Unit, Hammersmith Hospital, DuCane Road, London W12 OHS, UK.

active neurons release vasodilatory substances into the interstitial space that diffuse to local blood vessels and produce vasodilation. Many substances have been proposed as mediators of the local vascular response to neural activity [see Iadecola, 1993, for a review]. The most recent candidate is Nitric Oxide (NO) [Gally et al., 1990]. The current evidence implicating NO in the regulation of activity-dependent hemodynamics is diverse and compelling:

Endothelium-dependent vasodilation in response to acetylcholine was first demonstrated by Furchgott and Zawadski [1980]. Subsequently it has been shown that a number of substances can elicit vasodilation by inducing the release of endothelium-derived relaxing factor (EDRF). NO accounts for the action of EDRF and is formed by metabolism of L-arginine to NO and citrulline. The enzymes responsible have been identified in several tissues including the brain. NO synthase (NOS) is present in endothelial cells as well as perivascular nerves innervating large cerebral arteries. In neocortex NOS-containing neurons have a large number of processes which form an intricate network; ultrastructural studies have shown that the processes of NOS neurons are closely associated with intracerebral arterioles and capillaries [Iadecola et al., 1993]. These studies are based on immunocytochemical studies using antibodies raised against NOS or have employed NADPH-diaphorase as a marker of NOS [e.g. Bredt et al., 1990; Iadecola et al., 1993; and see Vincent and Hope, 1992].

There is a substantial amount of physiological evidence implicating NO as a mediator of local changes in perfusion [e.g. Cederqvist et al., 1991]. Modulation of blood flow by inhibitors of endogenous NO production has now been demonstrated in several preparations including isolated cerebral vessels [Gonzalez and Estrada, 1991] and the intact brain [e.g. Tanaka et al., 1991]. NO participates in the cerebral perfusion increases, elicited by stimulation of peripheral nerves: Northington et al. [1992] demonstrated that an NOS antagonist (L-nitroarginine-methyl-ester) blocked the cortical blood flow response to sciatic nerve stimulation in rats. Dirnagl et al. [1993] demonstrated that topical and systemic application of L-nitroarginine reduced the cerebral blood flow response to vibrissae stimulation by 50% in contralateral somatosensory cortex. Furthermore excitation of cortical neurons by topical application of the glutamate agonist NMDA produces a vasodilation that is reversibly attenuated by NOS inhibitors [Faraci and Breese, 1993]. Irikura et al., [1994] have shown that L-nitroarginine-induced attenuation, in barrel field blood flow, correlates with the inhibition of NOS activity assayed in homogenates taken from gray matter. They take this to suggest that NO generated from parenchymal NOS activity plays an important role in the cerebrovascular response to somatosensory stimulation.

The time-course of hemodynamic responses to changes in neural activity

The anatomy and physiology of cerebral perfusion is a complicated area that has been studied with new imaging techniques such as videomicroscopy, optical imaging and fMRI. For example direct videomicroscopy of cerebral vasculature in mouse barrel cortex reveals extensive collateralization of pial arteries. This surface vasculature gives rise to intra-cortical arterioles every 100–500 μm or so. The diameters of these arterioles are about 5–40 μm [Rovainen et al., 1991]. In cerebral cortex arterioles penetrate the brain substance up to layer 4, giving rise to smaller arterioles and capillaries. Intra-cerebral arterioles have a lining of smooth muscle cells that are replaced by pericytes in cerebral capillaries. Endothelial cells and pericytes are contractile cells that may relax via cGMP-mediated mechanisms [Iadecola, 1993].

In vivo optical imaging (of microcirculatory events) in visual cortex of monkeys has characterized the timing of activity-dependent changes [Frostig et al., 1990]. The data suggest the following sequence of events following a brief sensory stimulus: first, 200–400 ms after the onset of neural activity, highly localized oxygen delivery occurs followed 300–400 ms later by an increase in blood volume. After a second or more a substantial rise in local oxyhemoglobin is seen. With sustained stimulation intrinsic optical signals from rat barrel cortex have been observed to peak after several seconds [Masino et al., 1993].

These observations are consistent with both Doppler ultrasonography and fMRI data obtained during sensorimotor stimulation in human subjects: The transient nature of the fMRI hemodynamic response is usually attributed to a physiological uncoupling of regional cerebral perfusion and oxygen metabolism [Fox et al., 1988]. The result is a time-dependent change in the relative amounts of venous oxy- and deoxy-hemoglobin. Due to the differential magnetic susceptibility of oxy- and deoxy-hemoglobin, a transient change in intra-voxel dephasing is observed. This change underlies the measured signal [Kwong et al., 1992; Ogawa et al., 1992; Bandettini et al., 1992]. These data suggest a rise in relative oxyhemoglobin

that peaks at 4–8 s [Bandettini, 1993; Friston et al., 1994] and concur with the slower components of changes in intrinsic signals obtained with optical imaging [Frostig et al., 1990; Masino et al., 1993].

Conrad and Klingelhofer [1989] have used transcranial Doppler ultrasonography to measure the dynamics of local perfusion in occipital lobes during visual stimulation with stimuli of increasing complexity. They noted that it takes about 2 s for flow to reach 50% of maximal velocity after the onset of stimulation. This is in good agreement with time-courses above.

Constraints on diffusion

The physiological mechanisms that mediate between neural activity and hemodynamics are not, at the present time, fully known. However the empirical observations above provide constraints on the properties of substances that could act as diffusing spatial signals. In particular the fast time course of the activity-dependent hemodynamic response places a lower limit on the apparent rates of diffusion and elimination. Using simulations of microdiffusion we examined these constraints in terms of the time-constants of changes in the signal's concentration. These simulations were based on the assumption that some early component of activity-dependent hemodynamic response is mediated by signals that diffuse from the site of neural activity to the microvessels. To ensure the effective transduction of this signal the time-constants at the site of action should be about 400 ms or less. By examining the impact of diffusion geometry, apparent diffusion and elimination on these time-constants we estimated lower limits on apparent diffusion and elimination. As a result we were able to exclude some candidates for hemodynamic regulation, while demonstrating the sufficiency of others, notably NO.

METHODS

The model

It is assumed that an activity-dependent signal arises (directly or indirectly) in synaptic specializations or varicosities. There are about 300 million synapses per mm^3 of cerebral cortex [Shepherd and Koch, 1990]. One to two percent of cortical neurons stain for NOS. The contribution of these neurons to the synaptic population is unknown, but if it is proportional to the ratio of cell bodies 1–2% of synapses would be capable of originating a diffusible signal. In this case the average distance between the signal sources would be in the order of 10 μm. In rat cerebral cortex the density of varicosities on NOS/NADPH-diaphorase neurons is 15,000 per mm^2 [Iadecola, 1993]. This density again corresponds to an average separation of about 10 μm [for comparison; if one supposed that aminergic neurotransmitters could act as diffusible signals then the sources (varicosities and synaptic specializations of monoaminergic neurons) would be about 25–100 μm apart] [see Descarries et al., 1991].

In what follows the changes in signal concentration, seen by an arteriole, are modelled by changes at a point in a volume containing multiple sources with an appropriate distribution. The source geometry modelled in this paper was a distribution of point sources on the nodes of an infinitely large rectangular lattice. This geometry was chosen for mathematical expediency (see below). The primary focus of this model was the dynamics of concentration changes; the microvessels themselves were not explicitly modeled.

Because of the complicated spatiotemporal changes in signal concentration due to diffusion, the time-constants of these changes will vary considerably from point to point. After a transient increase in activity-dependent signal, points (arterioles) near a source will experience a rapid rise, followed by a relatively fast fall in concentration. The mechanisms contributing to the fall in concentration are 1 elimination and 2 diffusive dispersion of the signal. Conversely, arterioles that are remotely located from any source will have a slower onset and offset (and lower amplitude) due to the effects of signal dispersion. Figure 1 demonstrates these differences by depicting concentration profiles over time. Initially two sources produce a given amount of substance (the two peaks on the left) which diffuses into the surrounding space dispersing the signal and reducing the concentration gradients. Note that rate of concentration changes are acute near the sources but are more protracted in the intervening spaces. These data were produced using the algorithms described below.

The fast component of the hemodynamic response (200–400 ms) suggests a lower limit on apparent diffusion (D') and rate constant of elimination (k). These limits were estimated by calculating the concentration at time t (C_t) following instantaneous signal production at multiple discrete sources, giving an initial distribution (C_0). The profile of time-dependent changes in C_t were then used to calculate the rise

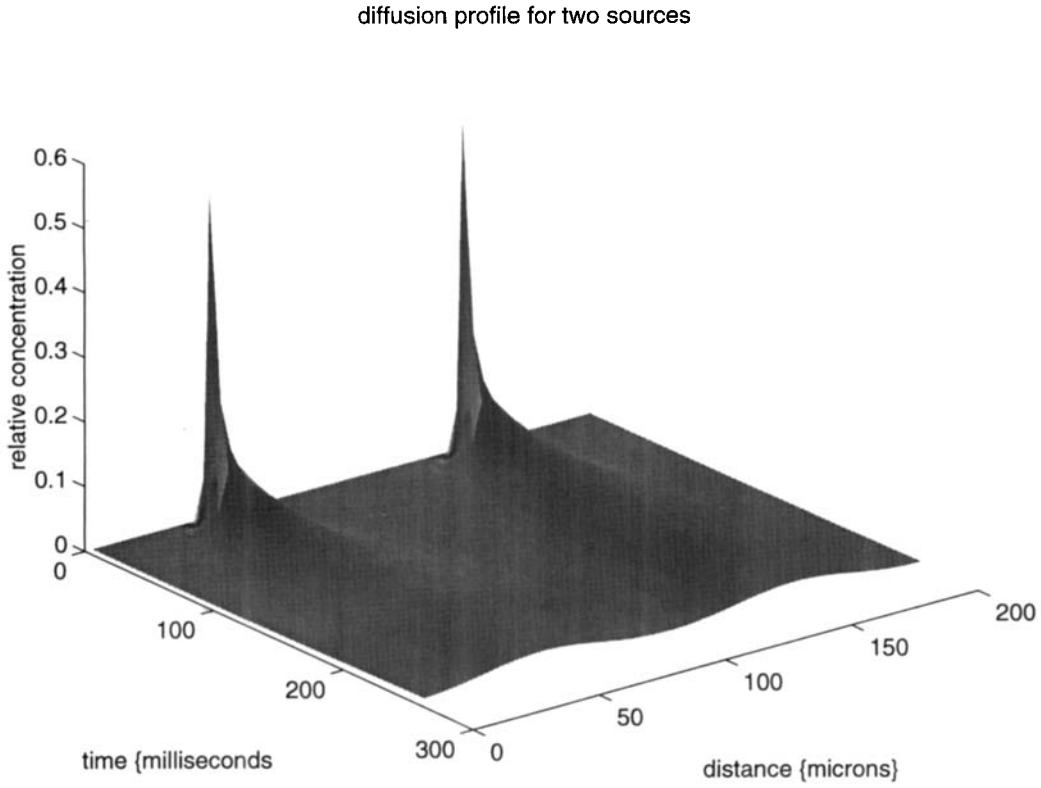

Figure 1.
Profile of one-dimensional diffusion from two point sources. Time proceeds from left to right. This profile is illustrative and the units are arbitrary. The point to note is that the time taken for concentration (height) to reach a maximum, and the rates of decay, vary considerably with distance from a source. These dynamics are more protracted at greater distances from the sources.

(onset) and fall (offset) time-constants for each point. This profile is equivalent to the system's impulse response function at the point in question. The time-constants associated with an impulse response function represent the fastest changes that could be evoked by any input (i.e., changes in neural activity).

As the rise (onset) and fall (offset) in C_t are likely to depend differently on the various diffusion parameters, the onset (*ton*) and offset (*toff*) time-constants were assessed over ranges of these parameters (D', k and the initial geometry C_0). *ton* was defined as the time to peak concentration and *toff* as the subsequent time taken for the concentration to fall to half the peak value (see Fig. 2). The characterization of the concentration changes in terms of *ton* and *toff* is clearly arbitrary but sufficient for the purposes of this work. We made no assumptions about the absolute concentrations of the diffusing substance, in relation to their physiologic effects, but assume that the relative concentration should necessarily change at least as fast as the onset of the effect being mediated. Expectations for these time constants were obtained by averaging over the appropriate volumes (the volumes that microvessels might occupy).

Computational details

Calculations were performed on a (SUN) workstation using MatLab (Mathworks Inc, Sherborn, MA). Neural volumes were modelled using 6.25 μm to 0.62 μm cubic voxels. Voxel size was adjusted according to the spatial distribution of sources. The concentration at any time t is denoted by the three dimensional array C_t with a value for every voxel of the simulated volume. C_0 represents the initial concentration following production of signal at discrete point sources (each source was modeled a single voxel). Multiple sources were distributed uniformly on a rectangular lattice, with a density characterized by their separation (σ). A finite difference scheme was implemented based upon

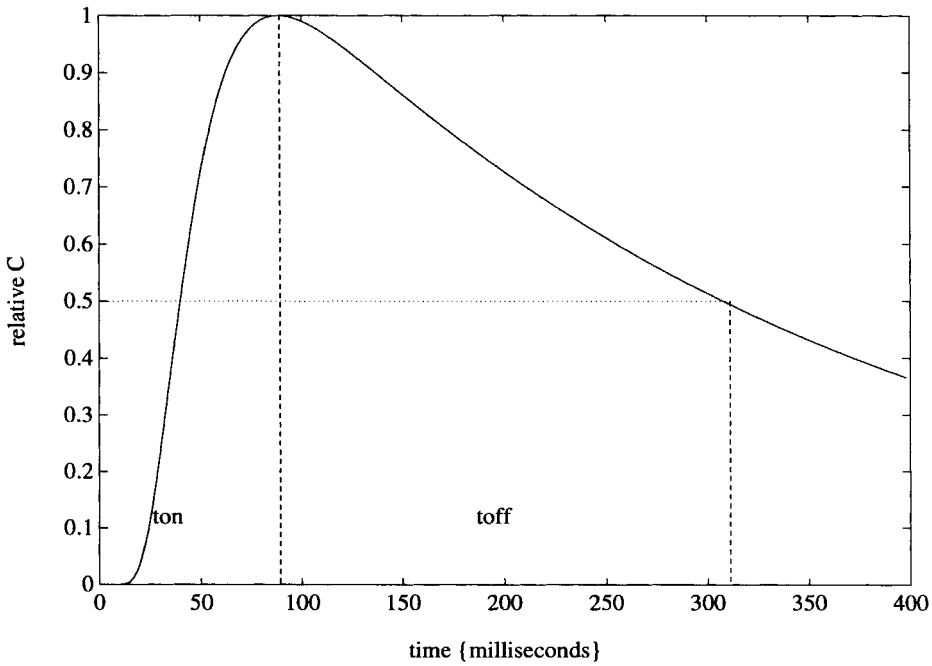

Figure 2.
Concentration changes over time at a single point. The parameters *ton* and *toff* refer to the time to reach maximum concentration and the time again to fall to half this level.

the standard differential equation for diffusion:

$$\partial C/\partial t = D'\nabla^2\{C\} - k \cdot C \qquad (1)$$

where $D' = D/\lambda^2$. λ is the tortuosity [Nicholson, 1985] associated with a specific substance and D is the diffusion constant. The effect of λ is to decrease the free diffusion (D) by an effect due to the convoluted shape of the extracellular volume, so that it can be described by an apparent diffusion coefficient (D'). The extracellular volume is like the soap phase of a foam of soap bubbles. Molecules restricted to this phase will have extended paths as they circumnavigate the intracellular compartment [Nicholson, 1985]. For substances confined to the extracellular compartment λ is typically about 1.6. For substances like NO that diffuse freely across membranes $\lambda = 1$. Implicit in Equation (1) is a first order elimination in a uniform fashion over the entire volume, with rate constant $k = \log(2)/t_{1/2}$ ($t_{1/2}$ is the half life). This is a reasonable assumption for the free radical NO that is oxidized rapidly throughout the parenchyma (but see Discussion).

Equation (1) was implemented by discretizing in space (voxels) and time (iterations) and reformulating Equation (1) in terms of convolution (*) with a diffusion kernel $I_{x,y,z}$ [Engstrom et al., 1988] where:

$$C_t = C_0 * I_{x,y,z} * I_{x,y,z} * \ldots\ldots\ldots * I_{x,y,z} \qquad (2)$$

for t convolutions. $I_{x,y,z}$ is zero apart from the voxel representing a source $I_{0,0,0} = 1 - 6.D' - k$ and the six juxtaposed voxels $I_{1,0,0} = I_{-1,0,0} = I_{0,1,0} = \ldots\ldots = I_{0,0,-1} = D'$. Equation (2) was implemented in Fourier space. Let $FT\{.\}$ denote Fourier transformation. Because convolution is the same as multiplication in Fourier space Equation (2) is equivalent to:

$$C_t = FT^{-1}\{FT\{C_0\} \cdot FT\{I_{x,y,z}\}^t\} \qquad (3)$$

The practical importance of Equation (3) is as follows: Formulation of the finite difference scheme in Fourier space means that periodic boundary conditions are implemented implicitly. Any elemental volume described by C_0 (and $I_{x,y,z}$) can be thought of as being replicated (to infinity) in all three dimensions. Therefore to simulate a lattice of uniformly distributed sources it is only necessary to compute Equation (3) for one source at the centre of its volume. The alternative approach would be to use the analytical solution of Equation (1) for one point source [see Nicholson and Rice, 1991] and simulate many point

sources with a lattice source geometry (the linearity of the convolution operator means that contributions from different sources can be simply summed). If one were able to compute the contributions from an infinite number of sources, the result would be the same as that obtained using Equation (3). Three dimensional Fast Fourier Transform algorithms were written in C. The elemental volume containing a single source was modelled by 16^3 cubic voxels. The initial value of C_0 at the voxel corresponding to the source $I_{0,0,0}$ was unity and zero elsewhere.

Simulations

The simulations were used to address two issues: 1) The sensitivity of the time-constants (*ton* and *toff*) to changes in source geometry (σ = distance between sources), apparent diffusion (D') and elimination ($t_{1/2}$); and 2) the sufficiency of candidate substances to act as diffusible signals, in particular NO.

The first simulations addressed the relationship between the diffusion parameters (σ, D' and $t_{1/2}$) and the time-constants for onset and offset of concentration changes, averaged over the whole volume (i.e. by assuming no particular spatial relationship between the location of microvessel receptor sites and the signal sources). Each diffusion parameter was varied while the remaining two were held constant, allowing the average *ton* and *toff* to be calculated as functions of source separation (σ), apparent diffusion (D') and elimination ($t_{1/2}$).

The results reported here are representative of the results for a variety of "fixed" values. The ranges of parameters examined were chosen to cover physiologically likely values. The ranges and constant values used are provided in Table I. For example the average spacing of NO-producing synapses is probably about 10 μm with a D' of 26×10^{-6} cm²/s and a half life of 100–1,000 ms. K^+ has a D' of 7.2×10^{-6} cm²/s with a half life of about 5 s [Paulson and Newman, 1987]. Most neurotransmitters have a D' of about 2×10^{-6} cm²/s, for example dopamine, 2.4×10^{-6} cm²/s [Nicholson and Rice, 1991]. Table II lists D' for several substances, including some implicated in the regulation of blood flow. The effects of changing these parameters, on *ton* and *toff* were presented graphically.

The second simulation tried to establish a rough lower limit on apparent diffusion in the context of sparse sources. This was estimated by assuming a "worst case scenario" based on the observation that arterioles can be 100 μm or more apart. Increases in neural activity may have to be communicated from regions interposed between arterioles within 200–400 ms. We therefore determined the lower limit on D' associated with a *ton* of 400 ms at 50 μm from the nearest source (the results of the first simulations above showed that *ton* was not greatly affected by elimination). This involved simulating sources 100 μm apart and looking at the concentration changes at points equidistant from those sources.

To do this the above simulations, for the effects of D' on *ton*, were repeated for sparsely distributed sources 100 μm apart. However the estimation of *ton* was restricted to planes halfway between sources. The shortest distance between any source and the plane of measurement was consequently 50 μm. Again the results were presented graphically showing *ton* as a function of D' for this source geometry.

TABLE I. Values of parameters used in the simulations

Name	Variable	Constant value	Range
Apparent diffusion	D'	8.1×10^{-6} cm²/s	$2–30 \times 10^{-6}$ cm²/s
Source separation	σ	20 μm	5–90 μm
Half life	$t_{1/2}$	200 ms	100 ms–2 s

RESULTS

The effect of changing diffusion parmeters on *ton* and *toff*

The effect of increasing source density was consistent, namely *ton* and *toff* increased with source separation σ. *ton* was relatively more sensitive to variation in

TABLE II. Apparent diffusion (D') 10^{-6} cm²/s at 25°C (in ascending order)

Hemoglobin	0.78
Ascorbate	2.2
Norepinephrine	2.2
5HT	2.2
Dopamine	2.4
Ca^{++}	3.0
K^+	7.2
Valine	8.3
O_2	16.0
CO_2	19.2
NO	26.0

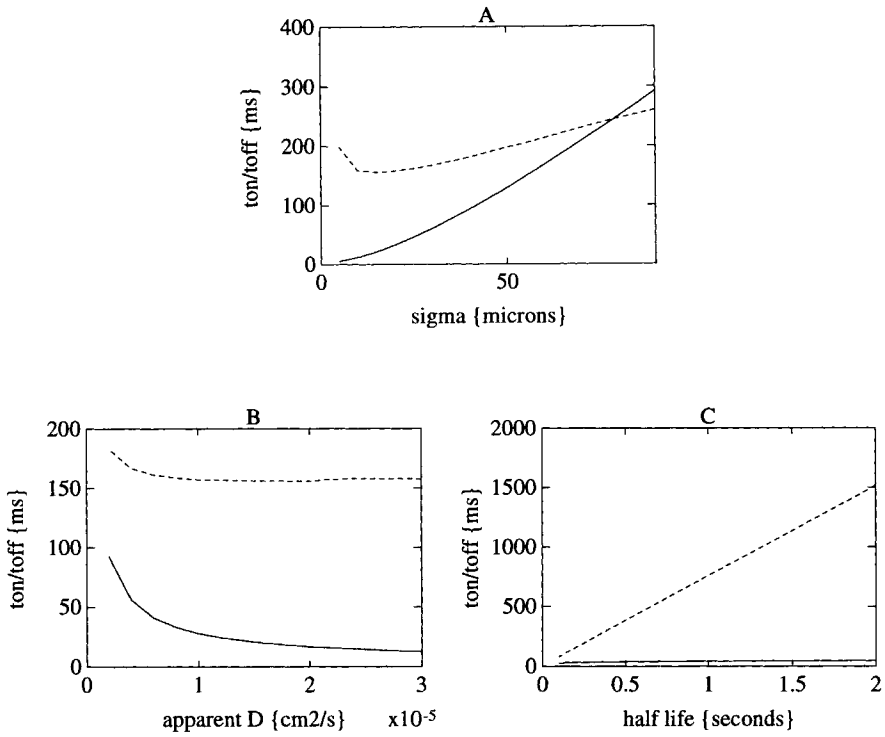

Figure 3.

Times to onset (*ton*, solid lines) and offset (*toff*, broken lines) of peak concentrations averaged over a volume containing uniformly distributed point sources. **A:** *ton* and *toff* as functions of source separation (σ) with constant apparent diffusion ($D' = 8.1\ 10^{-6}$ cm^2/s) and half life ($t_{1/2} = 200$ ms). **B:** *ton* and *toff* as functions of D' with constant $\sigma = 20$ μm and $t_{1/2} = 200$ ms. **C:** *ton* and *toff* as functions of $t_{1/2}$ with constant $\sigma = 20$ μm and $D' = 8.1 \times 10^{-6}$ cm^2/s).

source geometry than *toff* (see Figure 3A). The effects on *toff* were however quite interesting: At very small values of σ (e.g. 2 μm) values of *toff* tend to $t_{1/2}$. Increasing σ to about 10 μm reduces the apparent half life as elimination is augmented by local dispersion. This augmentation falls off with further separation due to the more protracted time courses in remote regions. As a result *toff* rises again and continues to rise above $t_{1/2}$ for very sparse distributions. The optimum σ that minimizes *toff* is around 10 μm, a similar value to that estimated for sources of NO in cerebral cortex.

Increasing D' reduced *ton* dramatically with a similar but less marked effect on *toff*. Conversely *toff* was very sensitive to changes in elimination, increasing almost linearly with $t_{1/2}$. *ton* was relatively unaffected. Figures 3B and 3C demonstrate this double dissociation.

In conclusion the time of onset of a microdiffusing signal is determined almost entirely by source geometry and apparent diffusion. Conversely, to a large extent, the offset is a function of elimination of the signal from tissue with a subtle [nonmonotonic] dependence on the spatial distribution of sources.

Lower limits on apparent diffusion for sparse sources

The lower limit on D' associated with a *ton* of less than 400 ms at 50 μm was about 21×10^{-6} cm^2/s (see Fig. 4). This relatively high value is exhibited by some gases, notably NO (see Table II). The peak concentrations attained in remote regions were about 0.14% of the peak concentration at source. However for substances with much smaller apparent diffusions (e.g. 4×10^{-6} cm^2/s) the peaks reached at around 50 μm were less than 10^{-7} of the initial source concentration.

In conclusion, according to the criterion that a microdiffusing signal must be effective within 400 ms over 50 μm (and under the current model assumptions), the only candidate for signalling neural activity to microvessels by passive diffusion is NO or a similar low molecular weight gas.

DISCUSSION

The hemodynamic response to the onset of neural activity shows many phases, ranging from a fast

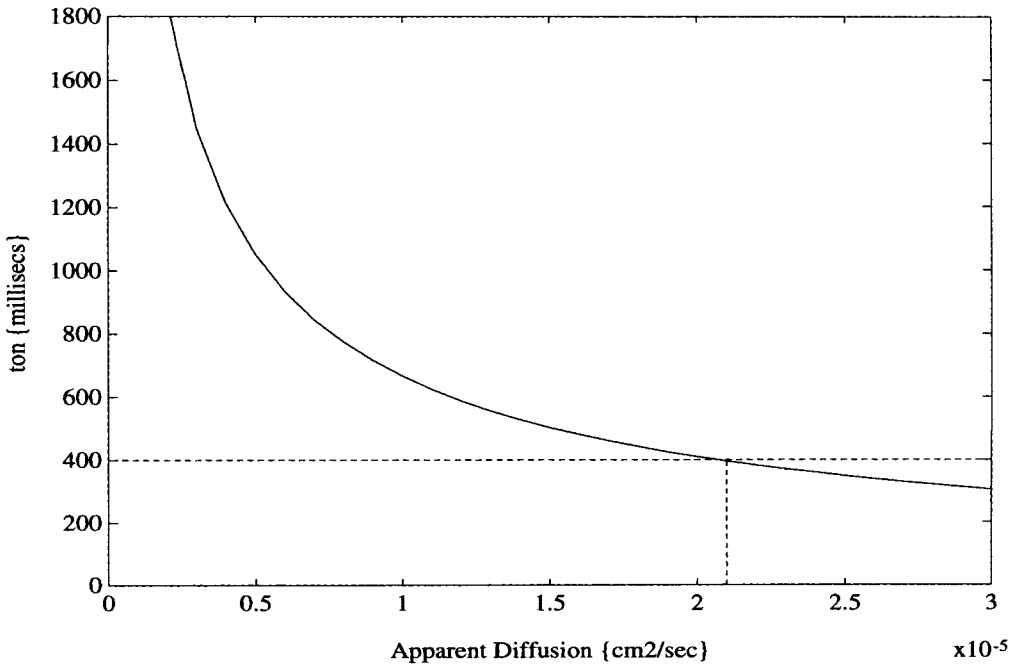

Figure 4.
ton in regions equidistant from sparse sources (σ = 100 μm), as a function of apparent diffusion ($t_{1/2}$ = 200 ms).

(200–400 ms) increase in oxygen delivery [Frostig et al., 1990] to slow (4–8 s) changes in the relative amounts of venous oxy and deoxy-hemoglobin as measured with functional MRI. This work has focussed on the fast component, asking "what are the necessary biophysical properties required of a substance to signal changes in neural activity, to the microvessels, by passive diffusion?" This question was addressed using a simple, but reasonable, analysis of time-dependent concentration changes at points in a volume of discrete sources. The analysis suggested that the apparent diffusion of NO is sufficiently high for it to act as a diffusible signal mediating activity-dependent changes in hemodynamics. This conclusion was based on simulations of the concentration changes throughout the tissue volume following activity-dependent production of a signal at discrete and sparsely distributed sources. A lower limit on apparent diffusion was established by noting that the largest distance a diffusible signal would have to diffuse is about 50 μm and that the time-constants for increases in concentration at the site of action should be less than 400 ms. This lower limit was about 21 × 10^{-6} cm^2/s. NO has an apparent diffusion of 26 × 10^{-6} cm^2/s.

The simulations also revealed a more general dependency of concentration dynamics on diffusion parameters. The time-constants for the rise in concentration were determined almost entirely by the source geometry (sparseness) and apparent diffusion. Conversely the offset time-constants depended most markedly on elimination rates. This double dissociation can result in a highly asymmetric rise and fall in concentration.

NO has been found to mediate a large number of diverse physiologic functions in many organs including the brain [Edelman and Gally, 1993]. Our analysis pointed to NO as the only candidate with a sufficiently high diffusion to act as a passively diffusing signal of fast activity-dependent changes. This is particularly relevant given that 1) NO can be identified with endothelium-derived releasing factor and 2) its production by NO synthase is activity-dependent [Garthwaite et al., 1988]. Garthwaite established a possible role for NO in the CNS by showing cerebellar neurons synthesize NO in response to excitatory neurotransmitters. Bredt and Snyder [1992] isolated and characterized NO synthase, now known to be endowed with NADPH-diaphorase activity [Vincent and Hope, 1992] and investigated its distribution throughout the CNS. The short half-life (NO is a free radical and is rapidly oxidized) and high diffusibility of NO uniquely qualify it to act as a spatial signal in the CNS. This role as a spatial signal is central to the NO hypothesis [Gally et al., 1990]. One component of the NO hypothesis is that activity-dependent NO production and its subsequent passive diffusion serve

to couple local changes in neural activity and perfusion.

The possibility that NO mediates some fast component of the activity-dependent hemodynamic response does not preclude other mechanisms or detract from the importance of the slower phases. "Although NO appears to be required for some neurally mediated increases in cerebral blood flow to occur, NO is unlikely to be the sole mediator.... In particular the mechanisms for upstream propagation of vasodilation to resistance vessels are likely to involve other agents" [Iadecola, 1993] or other mechanisms. Clearly neurogenic and active transport mechanisms constitute other important possibilities. For example Paulson and Newman [1987] have explored the possibility that potassium ions could be "siphoned" from the extracellular space by astrocytes and released from astrocyte endfeet (that abut against microvessels) to regulate changes in blood flow. Without this augmentation by "spatial buffering" the apparent diffusion of K^+ is too slow to account for the early phases of the hemodynamic response (recent evidence following the application of K^+ channel blockers argues against this spatial buffering hypothesis). The D' for K^+ (7.2×10^{-6} cm^2/s) suggests a rise time (at 50 μm from source) of 800 ms or more in our model (the elimination of K^+ is considerably slower than for NO). Passive diffusion might therefore be sufficient for K^+ to contribute the the intermediate and late phases of the hemodynamic response.

The model employed in this work does not incorporate many details which may or may not be important. For example we have made no attempt to explicitly model changes in elimination that may be a function of position either within or around the microvessels; the perivascular differences in the partial pressure of oxygen [see Ellsworth et al., 1994] may affect the oxidation of NO and introduce a spatial dependency in elimination constants (Constantino Iadecola—personal communication). An increasing role for biophysical models in addressing hypotheses about the mechanisms of cerebral hemodynamics and metabolism can be anticipated. The model presented here is possibly the simplest imaginable and yet has provided some useful, if provisional, insights.

ACKNOWLEDGMENTS

KJF is funded by the Wellcome Trust. Many thanks to Constantino Iadecola, Ron Frostig and Joseph Gally for very helpful discussions, comments and ideas. Some of this work was carried out as part of the Institute Fellows in Theoretical Neurobiology research program at The Neurosciences Institute, which is supported by the Neurosciences Research Foundation. The Foundation receives major support for this research from the J.D. and C.T. MacArthur Foundation, the Lucille P. Markey Charitable Trust. KJF was a W.M. Keck Foundation Fellow.

REFERENCES

Bandettini PA (1993): MRI studies of brain activation: Temporal characteristics. In: Functional MRI of the Brain. Berkeley, CA: Society of Magnetic Resonance in Medicine, pp 143–151.

Bandettini PA, Wong EC, Hinks RS, Tikofsky RS, Hyde JS (1992): Time course EPI of human brain function during task activation. Magn Reson Med 25:390–397.

Bredt DS, Snyder SH (1992): Nitric oxide, a novel neuronal messenger. Neuron 8:3–11.

Bredt DS, Hwang PM, Snyder SH (1990): Localization of nitric oxide synthase indicating a neural role for nitric oxide. Nature 347:768–770.

Cederqvist B, Wilund NP, Persson MG, Gustafsson LE (1991): Modulation of neuroeffector transmission in the guinea pig pulmonary artery by endogenous nitric oxide. Neurosci Lett 127:67–69.

Conrad B, Klingelhofer J (1989): Dynamics of regional cerebral blood flow for various visual stimuli. Exp Brain Res 77:437–441.

Descarries L, Seguela P, Watkins KC (1991): Nonjunctional relationships of monoamine axon terminals in the cerebral cortex of adult rat. In: Fuxe K, Agnati LF (eds): Volume Transmission in the Brain: Novel Mechanisms for Neural Transmission. New York: Raven, pp 53–62.

Dirnagl U, Lindauer U, Villiringer A (1993): Role of nitric oxide in the coupling of cerebral blood flow to neuronal activation in rats. Neurosci Lett 149:43–46.

Edelman GM, Gally JA (1993): Nitric oxide: Linking time and space in the brain. Proc Natl Acad Sci USA 89:11651–11652.

Ellsworth ML, Ellis CG, Popel AS, Pittman RN (1994): Role of microvessels in oxygen supply to tissue. NIPS 9:119–123.

Engstrom RC, Wightman RM, Kristensen EW (1988): Diffusional distortion in the monitoring of dynamic events. Anal Chem 60:652–656.

Faraci FM, Breese KR (1993): Nitric oxide mediates vasodilation in response to activation of N-methyl-D-aspartate receptors in the brain. Circ Res 72:476–480.

Fox PT, Raichle ME, Mintun MA, Dence C (1988): Nonoxidative glucose consumption during focal physiologic neural activity. Science 241:462–464.

Friston KJ, Jezzard P, Turner R (1994): Analysis of MRI time-series. Hum Brain Mapp 2:1–19.

Frostig RD, Lieke EE, Ts'o DY, Grinvald A (1990): Cortical functional architecture and local coupling between neuronal activity and the microcirculation revealed by in vivo high-resolution optical imaging of intrinsic signals. Proc Natl Acad Sci USA 87:6082–6086.

Furchgott RF, Zawadski O (1980): The obligatory role of endothelial cells in the relaxation of arterial smooth muscle by acetylcholine. Nature 288:373–376.

Gally JA, Montague PR, Reeke GN, Edelman GM (1990): The NO hypothesis. Proc Natl Acad Sci USA 87:3547–3551.

Garthwaite J, Charles SL, Chess-William R (1988): Endothelium derived relaxing factor release on activation of NMDA receptors

suggests role as intercellular messenger in the brain. Nature 336:385–388.

Gonzalez C, Estrada C (1991): Nitric oxide mediates the neurogenic vasodilation of bovine cerebral arteries. J Cereb Blood Flow Metab 11:366–370.

Iadecola C (1993): Regulation of the cerebral microcirculation during neural activity: Is nitric oxide the missing link? Trends Neurosci 16:206–214.

Iadecola C, Beitz AJ, Renno W, Xu X, Mayer B, Zhang F (1993): Nitric oxide synthase-containing neural processes on large cerebral arteries and cerebral microvessels. Brain Res 606:148–155.

Irikura K, Maynard KI, Moskowitz MA (1994): Importance of nitric oxide synthase inhibition to the attenuated vascular responses induced by topical L-nitroarginine during vibrissal stimulation. J Cereb Blood Flow Metab 14:45–48.

Kwong KK, Belliveau JW, Chesler DA, Goldberg IE, Weisskoff RM, Poncelet BP, Kennedy DN, Poncelet BP, Kennedy DN, Hoppel BE, Cohen MS, Turner R, Cheng HM, Brady TJ, Rosen BR (1992): Dynamic magnetic resonance imaging of human brain activity during primary sensory stimulation. Proc Natl Acad Sci USA 89:5675–5679.

Masino SA, Kwon MC, Dory Y, Frostig RD (1993): Characterization of functional organization within rat barrel cortex using intrinsic signal optical imaging through a thinned skull. Proc Natl Acad Sci USA 90:9998–10002.

Nicholson C (1985): Diffusion from an injected volume of a substance in brain tissue with arbitrary volume fraction and tortuosity. Brain Res 333:325–329.

Nicholson C, Rice ME (1991): Diffusion of ions and transmitters in the brain cell microenvironment. In: Fuxe K, Agnati LF (eds): Volume Transmission in the Brain. New York: Raven, pp 279–294.

Northington PJ, Matherene GP, Berne RM (1992): Competitive inhibition of nitric oxide synthase prevents the cortical hyperemia associated with peripheral nerve stimulation. Proc Natl Acad Sci USA 89:6649–6652.

Ogawa S, Tank DW, Menon R, Ellermann JM, Kim SG, Merkle H, Ugurbil K (1992): Intrinsic signal changes accompanying sensory stimulation: Functional brain mapping with magnetic resonance imaging. Proc Natl Acad Sci USA 89:5951–5955.

Paulson OB, Newman EA (1987): Does the release of potassium from astrocyte endfeet regulate cerebral blood flow? Science 237:896–898.

Rovainen CM, Woolsey TA, Wang DB, Blocher N, Robinson O (1991): Direct videomicroscopy of developing cerebral blood vessels and flow in mouse barrel cortex. J Cereb Blood Flow Metab 11(suppl 2):S633.

Roy C, Sherrington C (1890): On the regulation of the blood supply of the brain. J Physiol 11:85–108.

Shepherd G, Koch C (1990): Introduction to synaptic circuits. In: Shepherd GM (ed): The Synaptic Organization of the Brain. London: Oxford University Press, pp 3.

Tanaka K, Gotoh F, Gomi S, Takashima S, Mihara B, Shirai T, Nogawa S, Nagata E (1991): Inhibition of nitric oxide synthesis induces a significant reduction in local cerebral blood flow in rat. Neurosci Lett 127:129–132.

Vincent SR, Hope BT (1992): Neurons that say NO. Trends Neurosci 15:108–113.